Analysis of a Constant-Input-Flow Hydraulic System

Abstract: An analysis of the system is discussed and its application to a paper form feeder carriage in a printer is described. A nonlinear differential equation is derived based on stated assumptions and lumped oil parameters. The equation is linearized and solutions for motor velocity and peak pressure, both versus time, are determined. The analytical results show the effect of system parameters on system acceleration, steady state volumetric efficiency, and peak pressure. A limited amount of experimental data has been collected and good correlation between theoretical prediction and experimental results for acceleration time and peak pressure has been achieved.

Introduction

Reliable design criteria for predicting the response of a hydraulic pump and motor system are necessary adjuncts to the development of hydraulic equipment. In the system described below, the dependence of system response on the relative magnitude of various system parameters will be shown. In several cases, these parameters depend upon performance characteristics of the components employed in the system. Therefore, specific components have been selected and these performance characteristics will be determined so that a complete analysis may be presented specifically for the acceleration condition.

A distributed parameter analysis, leading to partial differential equations with complex boundary conditions, is not necessarily required for application of the systems studied which are of practical importance. Instead, a lumped parameter analysis, based on the conclusions for the distributed parameter analysis, is developed. This analysis results in a nonlinear second order ordinary differential equation. The nonlinearity is the result of nonlinear pressure losses generated by the valve, and channeling. For many applications this equation may be linearized by assuming a straight line approximation for the valve and channeling pressure losses. Correlation between the linear analysis and the experimental results for several systems has been found to be exceedingly good.

The constant-input-flow system shown in Fig. 1 employs a constant-displacement pump and a constant-displacement motor. The pump and motor are of spur gear design. The analysis, however, is applicable to pumps and motors of different design if the performance and empirical data for the other components is substi-

tuted for the values obtained for spur gear components. The pump and motor used are 12-pitch, 12-tooth, 0.400-inch face-width gears, enclosed in a housing with 0.0005-to 0.0012-inch axial clearance and 0.0016- to 0.0026-inch diametral clearance.

The basic constant-input-flow system is composed of a constant-volumetric-displacement pump and motor and a three-way spool valve, interconnected as shown in Fig. 1. The pump is driven at a constant rotary speed by an electric motor and delivers a constant oil flow into channel 2. The valve is externally held in either an extreme left or an extreme right position. The extreme left position represents a by-pass position where the

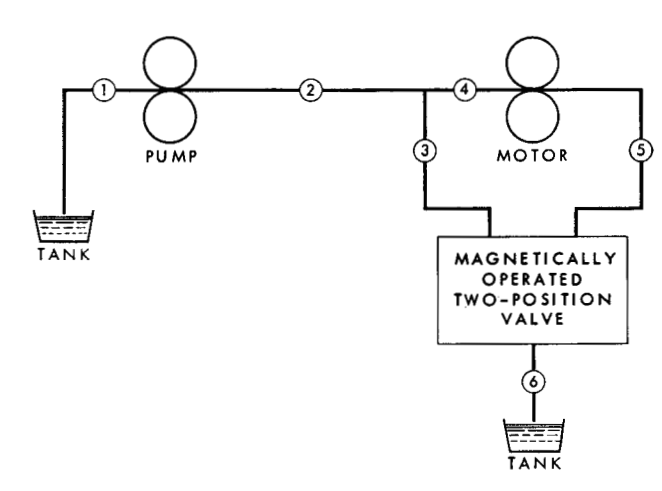


Figure 1 Constant input-flow hydraulic system uses a constant-displacement pump and a constant-displacement motor.

44

pump flow is directed to the reservoir through channels 3 and 6. At the same time, oil flow through the motor via channel 5 is blocked by the valve. The restriction to flow produced by the channeling and valves can be low with proper design. Therefore, the by-pass power loss of the system can be small.

A load motion cycle is started by transferring the valve to the extreme right position which simultaneously blocks the by-pass through channel 3 and opens the motor return path through channel 5. The combined effect of the motor inertia and the oil compliance generates a rapid pressure rise in the volume contained between pump outlet and the motor inlet. This pressure generates a large acceleration torque on the load. As the motor approaches the final motor velocity the pressure decays to a level sufficient to maintain the final motor velocity. Therefore the system has inherently provided a large acceleration pressure and a low steady state pressure. The motor will continue to turn at the final motor velocity until the valve is returned to the left position. The effect of this valve transfer is to open the by-pass and block the motor return path. The combined effect of the load inertia and the compliance of the oil generates a rapid pressure rise in the oil volume between the motor outlet and the valve. This pressure produces a large deceleration torque on the motor which rapidly brings the motor to rest.

Such a constant-input-flow hydraulic drive has been successfully applied as a drive for a paper form feed carriage, part of a printer. The hydraulic carriage drive operates as an on-off asynchronous clutch. The system is started by an electrical impulse to an electromagnetic valve drive from the printer. The paper is displaced the required number of line spaces at an output speed determined by the final motor speed. The stop signal comes from a commutator on the load shaft which is adjusted to a position which insures that the load will be in the correct location when finally at rest. A mechanical detent on the output shaft is used to prevent drift during printing.

The forms feed carriage and the apparatus used for the experimental portion of this paper employ an oilfilled reservoir in which the high-pressure components are completely submerged. This prevents any variation in performance that might result from air entrainment. Further, no high-pressure shaft seals are required on the pump or motor shafts. Low pressure seals are provided where the pump and motor shafts pass through the reservoir wall.

One useful application of the basic constant-input-flow system is for an on-off asynchronous clutch to displace a load a given number of discrete increments.

One advantage of the system is the inherent damping which produces smooth response and reduces stress in the related mechanical parts. This damping will be shown to result from component leakage and channeling losses.

Analysis

The following assumptions were made in the analysis of

the constant-input-flow hydraulic system shown in Fig. 1 and are based on experience with the design of such systems.

- Oil temperature, viscosity, density and bulk modulus are constant.
- 2. The channel losses are negligible in comparison to the valve losses.
- Pressure rise in the return line is independent of time.
- 4. The pump is driven at a constant input velocity.
- 5. Valve transfer is fast enough to have no effect on system response.
- The volume of oil between the pump outlet and motor inlet is contained in a single line between the elements.

The volumetric displacement of a spur gear pump and motor is a function of the design parameters of the internal gears. An empirical value of the displacement for the components under consideration may be found in Appendix I. The following fundamental relationships result from the volumetric displacement¹

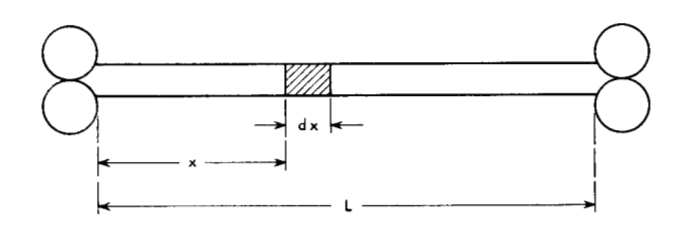
$$q = \omega d,$$
 (1)

$$T = Pd. (2)$$

Therefore, flow from the pump is a constant determined by the product of the constant drive velocity and the volumetric displacement; or

$$q_0 = \omega_0 d_0. \tag{3}$$

The relationship between the pressure and flow in the single line between the pump outlet and the motor inlet may be developed as follows based on the previous assumptions and based on the assumption that the particle



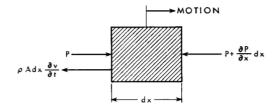


Figure 2 Forces acting on an element of hydraulic fluid between the pump outlet and motor inlet.

velocity and the pressure change are small enough to allow the product of these quantities and their derivatives to be negligible in comparison to first order terms. The sum of the forces acting on an element dx (as shown in Fig. 2) are

$$A[P-(P+\frac{\partial P}{\partial x}dx)] = \rho \frac{\partial v}{\partial t}Adx$$
, and $-\frac{\partial P}{\partial x} = \rho \frac{\partial v}{\partial t}$.

Applying the equation of continuity q=Av, and differentiating, we obtain $\frac{\partial q}{\partial t} = A \frac{\partial v}{\partial t}$.

Therefore

$$-\frac{\partial P}{\partial x} = P/A \frac{\partial q}{\partial t}.$$
 (4)

The equation relating the pressure change and the volume change for liquids neglecting thermal effect is

$$P_f - P_i = -\frac{B}{V_i} (V_f - V_i),$$

where the respective subscripts i and f are the initial and final conditions.

Differentiating this expression with respect to time we have

$$\frac{\partial V_f}{\partial t} = q = -\frac{V_i}{B} \frac{\partial P}{\partial t}$$
.

The net flow into the element dx is shown in Fig. 3 and results in the relationship

$$\frac{\partial P}{\partial t} = -\frac{B}{Adx} [q + \frac{\partial q}{\partial x} dx - q],$$

or

$$\frac{\partial P}{\partial t} = -\frac{B}{A} \frac{\partial q}{\partial x}.$$
 (5)

Successive differentiation and substitution of Eqs. (4) and (5) leads to the well known partial differential equations²

$$\frac{\partial^2 P}{\partial x^2} = \frac{1}{C^2} \frac{\partial^2 P}{\partial t^2},\tag{6}$$

and

$$\frac{\partial^2 q}{\partial x^2} = \frac{1}{C^2} \frac{\partial^2 q}{\partial t^2},\tag{7}$$

where $C^2 = B/\rho$.

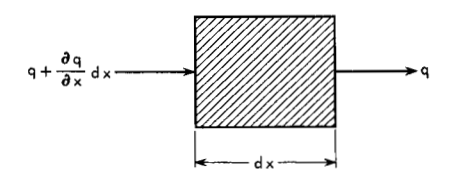


Figure 3 Net flow into element of hydraulic fluid.

The solution of these equations for the actual boundary conditions of the system being considered results in an expression which would be difficult to transform into the time domain. However, this complexity is unnecessary if one examines a few simplified cases. The first case of note is a closed channel with the valve by-pass line entering the main channel at the pump outlet. In this case, an instantaneous valve transfer may be represented as a step function of flow at the beginning of the channel. The solutions for pressure and flow as a function of displacement along the channel, and time, for this case are³

$$q(x,t) = q_0[N_1 - N_2],$$

and
$$P(x,t) = \frac{q_0 B}{AC} [N_1 + N_2],$$

where N_1 is such that

$$N_1=0$$
 if $t<\frac{X}{C}$,

$$(N_1-1)\frac{2L}{C} < t - \frac{X}{C} < N_1 \frac{2L}{C} \text{ if } t > \frac{X}{C},$$

and N_2 is such that

$$N_2=0$$
 if $t<\frac{2L-X}{C}$

$$(N_2-1)\frac{2L}{C} < t - \frac{2L-X}{C} < (N_2)\frac{2L}{C} \text{ if } t > \frac{2L-X}{C}.$$

The second case involves a closed channel with the valve close to the motor. In this case, an instantaneous valve transfer may be represented as a step function of flow at the end of the channel.

The solutions for pressure and flow as a function of displacement along the channel, and time, for this case are³

$$q(t,x) = q_0 + q_0[N_1 - N_2],$$

and

$$P(t,x) = \frac{q_0 B}{C A} [N_1 + N_2],$$

where N_1 is such that

$$N_1=0$$
 if $t<\frac{L+X}{C}$

$$(N_1-1)\frac{2L}{C} < t - \frac{L+X}{C} < N_1 \frac{2L}{C}$$
 if $t > \frac{L+X}{C}$,

and N_2 is such that

$$N_2=0$$
 if $t<\frac{L-X}{C}$,

$$(N_2-1)\frac{2L}{C} < t - \frac{L-X}{C} < N_2 \frac{2L}{C}$$
 if $t > \frac{L-X}{C}$.

The third case is a closed channel with the valve located at X=L/2. If the system is divided at X=L/2 into two

46

systems, the left-hand system will be the same as the second case and the right-hand system will be the same as the first case, with L/2 replacing L and the amplitudes equal to one-half of the values shown in cases 1 and 2.

Pressure is shown as a function time for the respective three cases of valve position at x equal to 0, L/2, and L in Figs. 4, 5 and 6.

Examination of these three cases indicates that an average value of pressure rise as a function of time, but independent of valve position and independent of the displacement along the channel, may be expressed as

$$\frac{dP}{dt} = \frac{q_0B}{CAt} = \frac{q_0B}{CA_C^L} = \frac{q_0B}{AC} = \frac{q_0B}{V_0}.$$

Neglecting the influence of the position along the line on the pressure at any point where the pressure is observed results in an error in time. The maximum time error possible is equal to τ , which is the length of the channel divided by the velocity of sound in the liquid. For a realistic channel length of four inches, and a velocity of sound of 50,000 in./sec., the value of τ is 0.08 milliseconds. It will be shown that the acceleration time for the practical system experimentally tested is from 2 to 50 milliseconds. Therefore, the maximum time variation from the average value resulting from the dependence of pressure upon the position along the line is 25 to 625 times less than the acceleration time.

It will be assumed then, that the effects of oil compliance are lumped rather than distributed. This means that the pressure rise in the channel is assumed to be independent of the position along the channel. Further, it will be assumed that the relationship between the pressure rise and input flow for the channel will equal the average value for the three cases studied, namely

$$q = \frac{V_1}{R} \cdot \frac{dP}{dt}.$$
 (8)

In equation (8), q is assumed to be the net sum of the flow into, and out of, the system. This assumption is based on the independence of pressure on location in the channel and the gradual change of the outflows on a time base equal to L/C or L/2C in the more practical case of a valve half way between the pump and the motor.

The two outflows from the system are the motor flow and the leakage flow. The motor flow is found from equation (1) to be

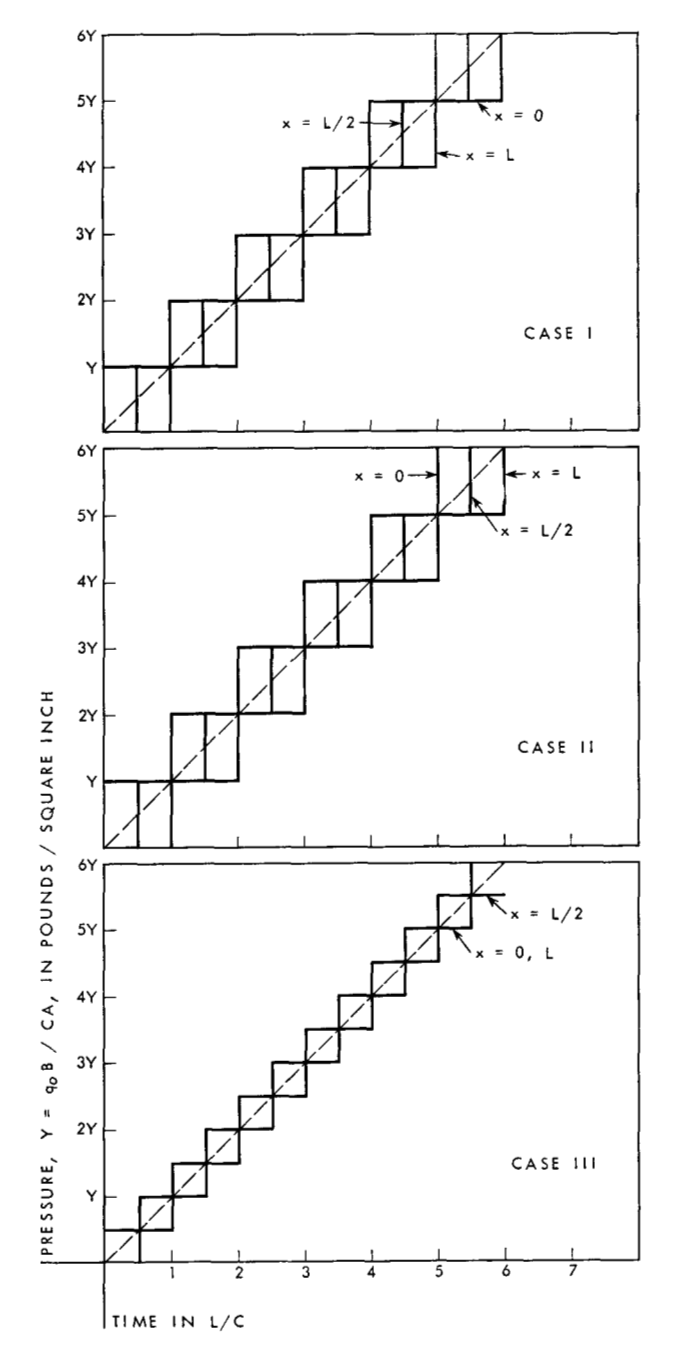
$$q_1 = \omega_1 d_1$$
.

The leakage flow of the pump and motor units under consideration is found empirically (Appendix III) to be

$$q_2 = M_1 P_1 + L_1 \omega_0 + Y$$

and

$$q_3 = M_2(P_1 - P_2) + L_2\omega_1 + Z.$$



Figures 4, 5 and 6
Pressure versus time for the three cases (see text).

Neglecting valve leakage, the net sum of the inflow and the outflow is

$$q = q_0 - (q_1 + q_2 + q_3). (9)$$

Substituting Eq. (9) into Eq. (8) we obtain

$$q_0 - (q_1 + q_2 + q_3) = \frac{V_1}{B} \frac{dP_1}{dt},$$

or

47

$$q_0 = \omega_1 d_1 + (M_1 + M_2) P_1 + L_1 \omega_0 + L_2 \omega_1$$

$$-M_2 P_2 + Y + Z + \frac{V_1}{B} \frac{dP_1}{dt}.$$
(10)

Equation (10) contains two dependent variables; the pressure in the input channel and the motor velocity. Input channel pressure is equal to the sum of the acceleration pressure and the pressure losses which have been assumed to be after the motor. The pressure losses may be divided into two parts; the motor friction loss, found to be a function of the motor velocity (Appendix II), and the valve losses which are a function of the square of the motor velocity. The acceleration pressure is found by Newton's Law and Eq. (2) to be a function of the first time derivative of the motor velocity. Hence, the pressure in the input channel is

$$P_1 = \frac{J}{d_1} \frac{d\omega_1}{dt} + P_2,$$

where

$$P_2 = P_{MF} + P_{VL} = K_1 \omega_1 + K_1 \omega_1^2$$

and

$$P_{MF} = K_1 \omega_1, \tag{11}$$

$$P_{VL} = K_1 \omega_1^2$$
.

Thus.

$$P_{1} = \frac{J}{d_{1}} \frac{d\omega_{1}}{dt} + K_{1}\omega + K_{2}\omega_{1}^{2}. \tag{11}$$

The first time derivative of P_1 is

$$\frac{dP_1}{dt} = \frac{J}{d_1} \frac{d^2\omega_1}{dt^2} + K_1 \frac{d\omega_1}{dt} + 2K_2\omega_1 \frac{d\omega_1}{dt}.$$
 (12)

The substitution of Eq. (11) and (12) into Eq. (10) results in a nonlinear ordinary differential equation of the second order (where motor velocity is a function of time)

$$q_{0} - (L_{1}\omega_{0} + Y + Z) = \frac{V_{1}J}{Bd_{1}} \frac{d^{2}\omega_{1}}{dt^{2}} + \left[\frac{(M_{1} + M_{2})J}{d_{1}} + \frac{V_{1}K_{1}}{B} + \frac{2K_{2}V_{1}\omega_{1}}{B} \right] \frac{d\omega_{1}}{dt} + (K_{1}M_{1}td_{1} + L_{2}M_{1}\omega_{1})\omega_{1}.$$
(13)

The motor velocity and its first time derivative equal zero at the instant of valve transfer, thus

$$\omega_1(0) = 0$$
, and $\frac{d\omega_1}{dt}(0) = 0$. (14)

Therefore, an ordinary differential equation describing the motor velocity as a function of time has been derived. The nonlinear coefficients in the motor velocity and the first time derivative terms in the expression for

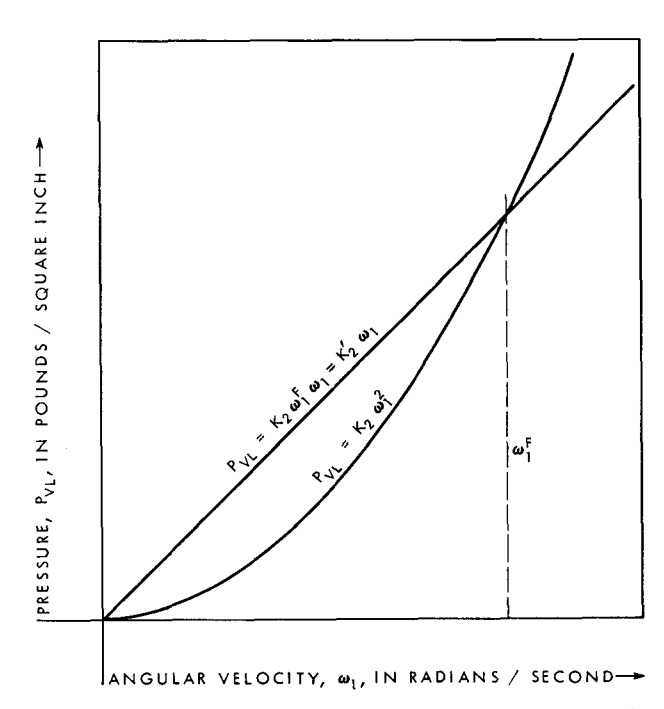


Figure 7 Effect of linearizing Equation 13 (see text).

motor velocity require a numerical solution. At the time when volume restrictions must be established, the advantages of a closed form solution for design criteria is apparent. If these nonlinear terms are small in comparison with the linear term to which they are added, K_2 may be assumed zero. However, for many systems the nonlinear terms are small but not negligible. Therefore it is now proposed that equation (13) be linearized by assuming that

$$P_{VL} = K_2 \omega_1^F \omega_1 = K_2' \omega_1 \tag{15}$$

where ω_1^F is the final motor velocity. The significance of this assumption is shown in Fig. 7. The effect of the nonlinear terms is overestimated when the motor velocity is below its final value and underestimated when it is above its final value. This assumption leads to the linear second order ordinary differential equation

$$q_{0} - (L_{1}\omega_{0} + Y + Z) = \frac{V_{1}J}{Bd_{1}} \frac{d^{2}\omega_{1}}{dt^{2}} + \left[\frac{(M_{1} + M_{2})J}{d_{1}} + \frac{V_{1}(K_{1} + K'_{2})}{B} \right] \frac{d\omega_{1}}{dt} + [(K_{1} + K'_{2})M_{1} + d_{1} + L_{2}]\omega_{1},$$
(16)

where

$$\omega_1(0) = 0$$
, and

$$\frac{d\omega_1}{dt}(0) = 0. ag{17}$$

The solution of this equation is simplified by using the following notation:

$$a = \frac{V_1 J}{B d_1},$$

$$b = \frac{(M_1 + M_2) J}{d_1} + \frac{V(K_1 + 2K'_2)}{B},$$

$$c = [(K_1 + K'_2) M_1 + d_1 + L_2],$$

$$f = q - (L_1 \omega_0 + Y + Z),$$

$$\omega_c = \sqrt{(c/a) - (b/2a)^2},$$

$$\omega_b = \sqrt{(b/2a)^2 - (c/a)},$$

$$\omega_d = b/2a,$$
and
$$\omega_1^F = f/c.$$

The solution of Eqs. (16) and (17) takes two basic forms depending upon whether ω_b or ω_c is real. If ω_c is real, the solution represents underdamped oscillations about the final motor velocity as shown in Figure 8a. The solution is

$$\omega = \omega_1^F [1 - e^{-\omega_s t} \{ (\cos ine \ \omega_c t) + \frac{\omega_d}{\omega_c} \sin e \ (\omega_c t) \}]. \tag{18}$$

For this case, we may define the acceleration time as the first time the motor velocity passes through its final velocity. This is found by equating the motor velocity to the final motor velocity in Eq. (18). The result for the first passage through the final motor velocity is

$$t = \frac{\pi/2 + \operatorname{tangent}^{-1}\left(\frac{\omega_d}{\omega_c}\right)}{\omega_c}.$$
 (19)

The relationship between the pressure and time is found by making the appropriate substitution of Eq. (18) into Eq. (11), after Eq. (11) has been linearized by the substitution of Eq. (15). The resulting equation for the case in question is

$$P_{1} = \left[\frac{J_{\omega_{t}^{F}}}{d_{1}\omega_{c}}\right] \left[c/a\right] \left[e^{-\omega_{d}t} \sin \omega_{c}t\right] + (K_{1} + K'_{2})\omega_{1}^{F} \left[1 - e^{-\omega_{d}t} \cos \omega_{c}t + \frac{\omega_{d}}{\omega_{c}} \sin \omega_{c}t\right]. (20)$$

The value of the peak pressure is important as a design parameter to insure the mechanical strength of the component parts. The time when the peak pressure occurs may be determined by differentiating Eq. (20), setting the result equal to zero and solving for the time. The result is

$$t_1 = \frac{1}{\omega_c} \tan^{-1} \left[\frac{R_1 \omega_c}{R_2 \left[\frac{\omega_d^2}{\omega_c} + \omega_c \right] - R_1 \omega_d} \right], \tag{21}$$

where

$$R_1 = \left[\frac{J\omega_1^F}{d_1\omega_c} \right] c/a$$
, and $R_2 = (K_1 + K'_2)\omega^F$.

General solutions similar to these given in Eqs. (18) and (20) may be found for the case when ω_b is real; these solutions represent an exponential rise to the final motor velocity (Fig. 8b). These are

$$\omega = \omega_1^F \left[1 - e^{-\omega_d t} \left(\cosh \omega_b t + \frac{\omega_d}{\omega_b} \sinh \omega_b t \right) \right], \tag{22}$$

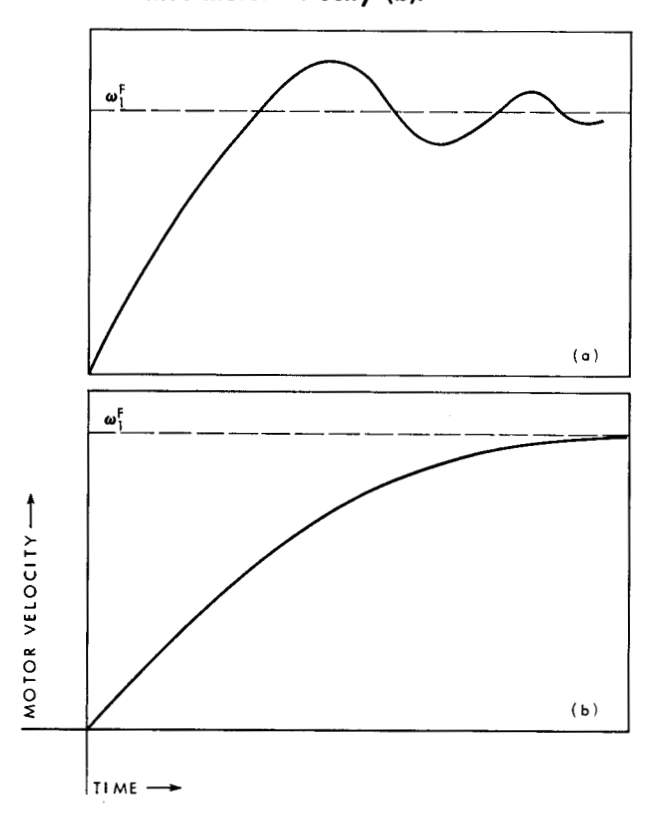
and

$$P_{1} = \left[\frac{J_{\omega_{1}^{F}}}{d_{1}\omega b}\right] \left[c/a\right] \left[e^{-\omega_{d}t} \sinh \omega_{b}t\right] + (K_{1} + K'_{2})\omega_{1}^{F} \left[1 - e^{-\omega_{d}t} \left(\cosh \omega_{b}t + \frac{\omega_{d}}{\omega_{b}} \sinh \omega_{b}t\right)\right].$$
(23)

A solution for the acceleration time similar to Eq. (19) is impractical in this case since the motor never reaches final velocity. A solution whose application is similar to equation (21) is found using

$$t_1 = \frac{1}{\omega_b} \tanh^{-1} \left[\frac{R_1 \omega_b}{R_2 \left[\frac{{\omega_d}^2}{\omega_b} - \omega_b \right] - R_1 \omega_d} \right],$$

Figure 8 Underdamped oscillations about final motor velocity (a) and exponential rise to final motor velocity (b).



where
$$R_1 = \left[\frac{J_{\omega_1^F}}{d_1 \omega_b} \right]$$
, and $R_2 = (K_1 + K'_2) \omega^F$.

The steady state volumetric efficiency of the system may be found by the equation

$$v\!=\!\frac{\omega_1^Fd_1}{q_0}\!=\!\frac{q_0\!-\!(L_1\omega_0\!+\!Y\!+\!Z)}{(q_0/d_1)[(K_1\!+\!K'_2)M_1\!+\!d_1\!+\!L_2]}.$$

Summarizing, a nonlinear differential equation has been derived based on the original assumptions and lumped oil parameters in the pump outlet to motor inlet channel. This equation has been linearized and solutions for motor velocity and peak pressure versus time have been determined. The response of the system depends on the load inertia (J), the system volume (V), the oil bulk modulus (B), the leakage coefficients (M, L, Y, Z), the friction coefficients (K_1+K_2') and the volumetric displacement of the pump and motor (d_0, d_1) . The final motor velocity does not affect the system acceleration time as defined by equation (19); however, it will affect the peak system pressure.

In this article, no mention of deceleration characteristics has been made. It can be shown that linearized differential equation (16) also defines the deceleration from a constant motor velocity ω_1^F to zero velocity if appropriate changes in the system constants are made. For the deceleration case V_1 in Eq. (16) is the volume enclosed between the motor outlet and the valve, and M_1 , L_1 , Y and K_2 in Eq. (16) are zero. The initial conditions for the deceleration case become $\omega_1(0) = \omega_1^F$ and $\frac{d}{dt}[\omega_1(0)]=0$. These changes allow the development of solutions similar to the solutions for the acceleration case.

Experimental data

A limited amount of experimental data has been collected to verify the theoretical results derived. The experiments were limited to a spur gear pump and a spur gear motor of 12-teeth, 12-pitch and 0.400-in. face width; the pump and motor displacements were not varied. The leakage coefficient of the pump and motor were varied by changing the axial and radial clearance between the gears and the housing in two steps, representing the maximum and minimum clearance for the production pump and motor units used. For design purposes the acceleration time for the maximum leakage or clearance conditions, and the peak pressure value for the minimum clearance condition must be used. The minimum clearance condition represents an axial gear clearance of 0.0005 in. and a radial gear clearance of 0.0008 in.; the maximum clearance condition: an axial gear clearance of 0.012 in. and a radial gear clearance of 0.0013 in.

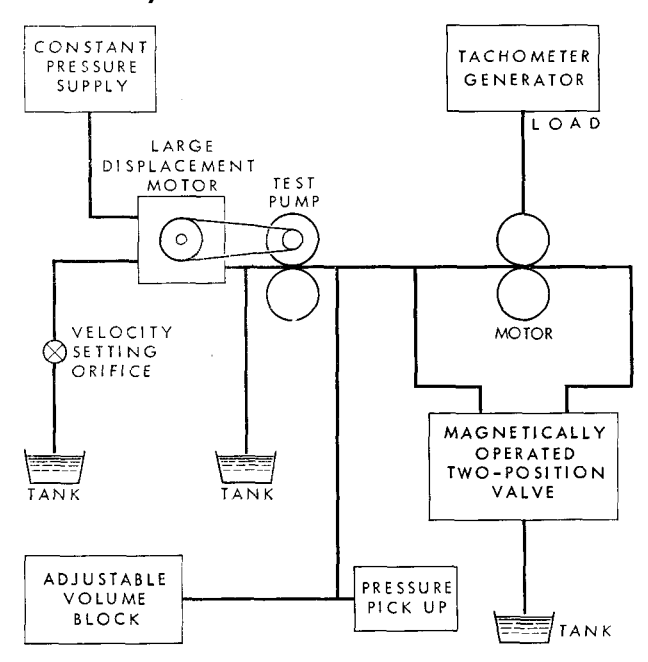
The load inertia was varied from 1.69×10^{-4} to 5.0×10^{-3} in-lb-sec² in four steps. This range was dictated by the motor size (i.e., loads smaller than 1.69×10^{-4} in-lb-sec², of which 0.84×10^{-4} in-lb-sec² is the motor itself, are impractical for the motor size; loads larger than

5.0×10⁻³ in-lb-sec² would require a larger volumetric displacement motor for efficient application). The volume contained between the pump outlet and the motor inlet was varied between 1.0 cubic inch and 2.5 cubic inches in three steps. This range was chosen as a practical one for the motor size. The final motor velocity was varied in two steps of 1,000 and 2,000 revolutions per minute. The oil bulk modulus was not varied because the use of petroleum base fluids is generally accepted and such fluids have a constant bulk modulus. The bulk modulus was determined experimentally (Appendix 4).

The selection of the range and increments for variation of the parameters was based on practical consideration of the possible applications of such systems as shown in Fig. 1 to limit the number of tests and still provide adequate demonstration of the analytical results. The load was varied by adding disks to the motor shaft and the volume was varied by adding additional chambers of oil to the volume enclosed between the pump outlet and the motor inlet. The pump drive system contained a large inertia hydraulic motor driven from a test stand power supply to allow variable velocity input with constant velocity regulation within 1 percent. For each test point, the final motor velocity was established for the type system desired.

The motor velocity was measured with a Kearfott tachometer generator, type 700-1A, using a 3,000 cycle-per-second input from an audio oscillator. The linearity of the tachometer generator used to measure the velocity was found to be unaffected at this frequency. The system pressure was measured with pressure pickup of the unbonded strain gage type. Signals from the two transducers were displayed on an oscilloscope, and the traces

Figure 9 Configuration of equipment used to test system characteristics.



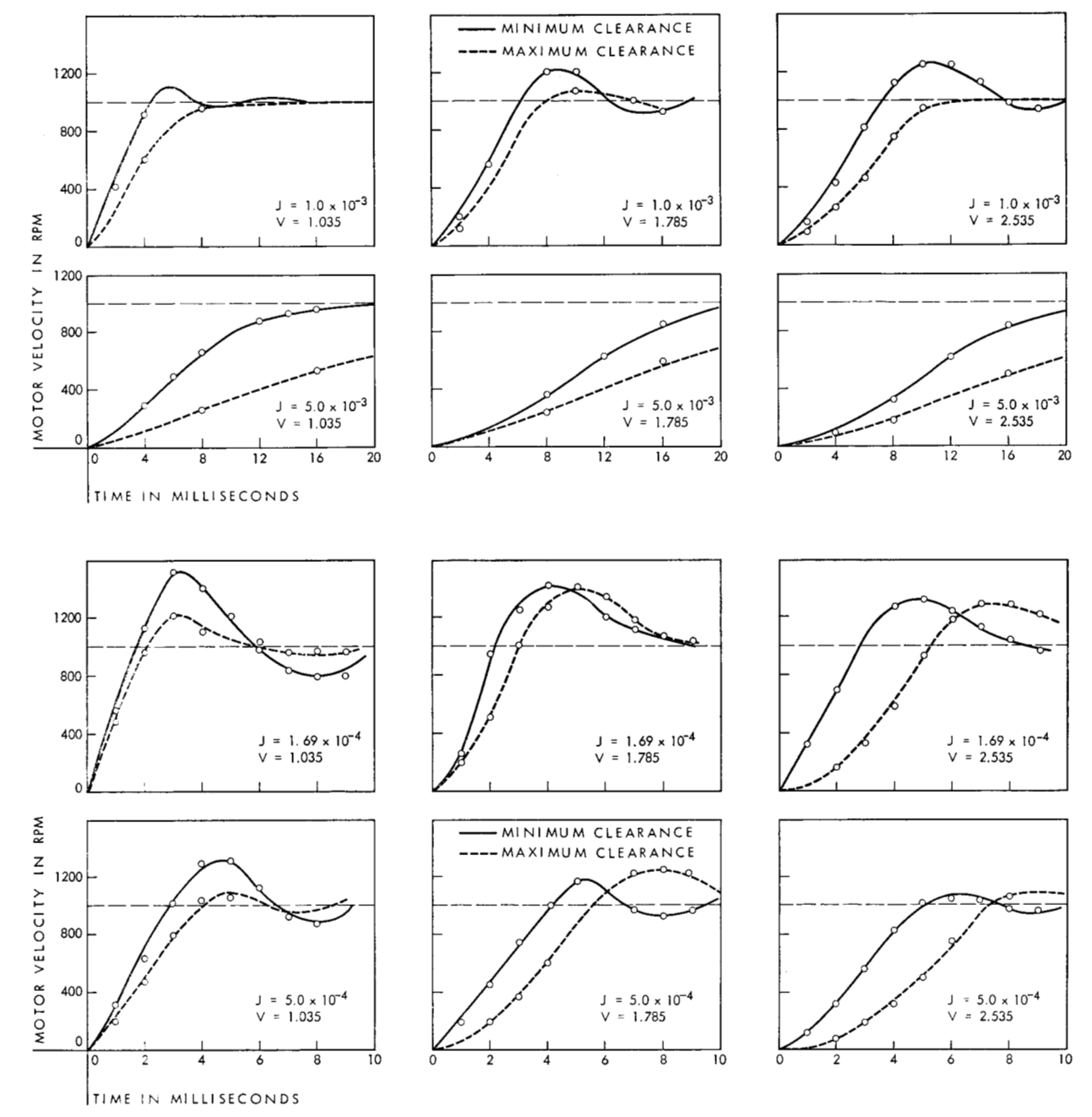


Figure 10 Motor velocity versus time for various parameters shown and with final motor velocity of 1,000 revolutions per minute.

were triggered from the start of valve motion. However, the acceleration time was measured from the beginning of motor rotation. This was done because the usual cyclic application for this type of clutch allows the magnet delay to be present into the previous cycle. The time and transducer amplitude scales were varied for each experiment to allow for the greatest reading accuracy of the desired result. The test configuration is shown schematically in Fig. 9.

Discussion of results

The motor velocity-vesus-time curves for the various parameters under consideration and 1,000 revolutions per minute final motor velocity are shown in Fig. 10. Each graph represents the motor velocity-versus-time curve for each inertia and volume condition with the effect of internal clearance change shown. Each row represents a given load with volume changing, and each column represents a given volume with load changing.

The results with 2,000 revolutions per minute final motor velocity are not shown because the values of acceleration time are defined by Eq. (19) and the shape of the curves are within 5 percent of the results shown for 1,000 revolutions per minute. The correlation between the actual acceleration time and the acceleration time predicted by Eq. (19) is shown in Fig. 11; here, actual and theoretical acceleration time for the 1,000 revolutions per minute cases are plotted against the underdamped frequency ω_c . The range results from the effect of increasing damping for a given ω_c . The comparison of actual and theoretical peak pressure is shown in Fig. 12.

The correlation between experimental and theoretical results is rather good for the limited amount of testing done. This in itself is verification of the assumptions made for the systems tested. However, the amount of nonlinear valve and channeling pressure losses present in the system tested was small. The total full speed pressure loss for this system was 100 pounds per square inch. Valve and channeling pressure losses must be limited to this value or less if the linearized differential equation solutions are to be used. It is apparent from the results that sufficient damping can be employed as the result of leakage so that channel and valve losses may be minimized.

Conclusions

The basic constant-input-flow hydraulic system described may be represented by a nonlinear ordinary differential equation of second order for those systems where response is slow enough to warrant the assumption that oil capacitance and inertia are lumped constants. Further, the equation may be linearized for systems where the velocity-squared pressure losses have been minimized. The resulting linearized differential equation has the form of a simple spring-mass system with viscous damping.

The motor velocity and pressure response resulting from a rapid valve transfer has been predicted with reasonable accuracy by the solution to the linearized differential equation for a limited amount of experimental data. The experimental set up was limited to a spur gear type of pump and motor of one size; thus, it is limited to the practical range of application of the other parameters in a system using this pump and motor size.

The analytical results indicate that future demands for faster response will require understanding of the effect of distributed parameters on the acceleration time. It is hoped then, that fundamental investigations of pressure wave propagation in hydraulic transmission lines will be the next step toward the advancement of constant-input-flow systems. The inherent advantage of a constant-input-flow system (varying power with load requirements, simple construction and inherent damping) promise faster and smooth responding clutches or positioning devices. Space considerations and valve transfer speed are presently the limiting factors in attaining faster response.

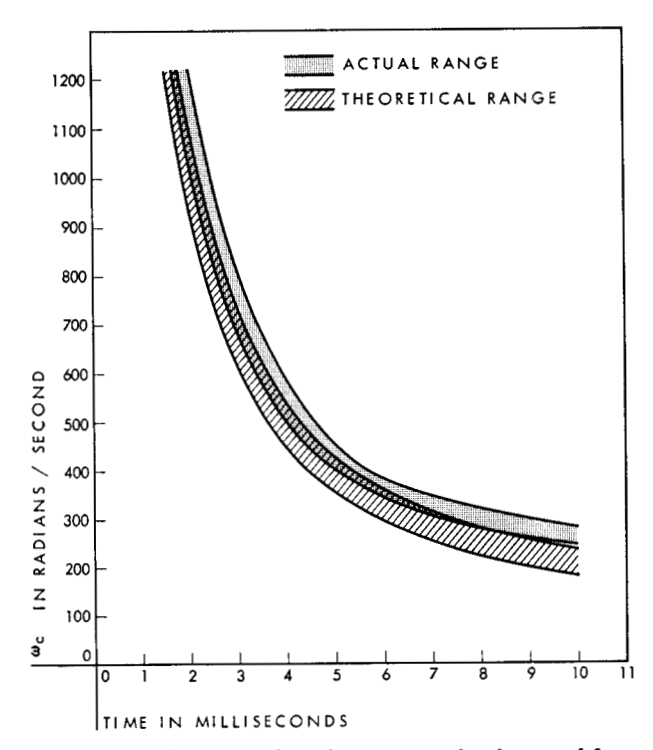


Figure 11 Theoretical and actual underdamped frequency versus acceleration time.

Appendix 1: Determination of volumetric displacement

The volumetric displacement of the pump and motor used for the experimental tests was determined by hand cranking the pump and motor against no restriction or pressure loss at very low velocity for a great number of revolutions. The result obtained for the pump was within 2 percent of that obtained for the motor; the average value obtained was

 $d_0 = d_1 = 0.0366 \text{ in}^3/\text{RAD}.$

Appendix II: Determination of the motor friction coefficient

This coefficient was determined by operating the motor against no external restriction or pressure and measuring the speed resulting from an incremental increase in inlet pressure. The results were plotted with pressure as the ordinate and motor velocity as the abscissa. Therefore the slope of the resulting linear curve is the desired motor friction coefficient. The value obtained is

$$K_1 = 0.227 \frac{\text{lb-sec}}{\text{in}^2}$$

Appendix III: Determination of the pump and motor leakage coefficients

The pump leakage relationship was determined by operating the pump against the restriction of a variable orifice. Measurements of the actual pump output flow

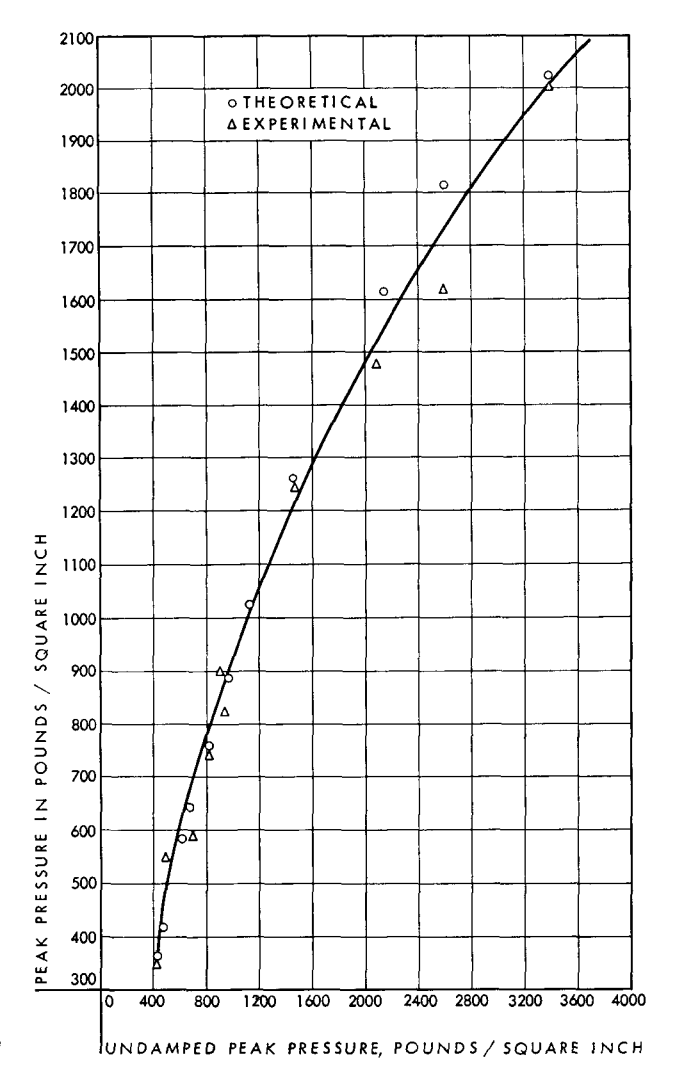


Figure 12 Theoretical and experimental comparison of peak pressure.

were taken for various pumps speeds and restriction pressures. The leakage flow was determined for each test point by subtracting the actual pump outlet flow from the theoretical output flow for the pump speed maintained during the test point.

The results indicate that the pump leakage flow is dependent upon the pump outlet pressure and the pump speed. The relationship, empirically determined was

$$q_2 = M_1 P_1 + L_1 \omega_0 + Y.$$

The motor leakage relationship was determined by operating the motor with an external source of pressure against an adjustable external source of load torque and speed. Measurements of the actual motor input flows were taken for various motor velocities and outlet torques. The leakage flow was determined for each test point by subtracting the theoretical motor inlet flow from the actual motor inlet flow for the motor velocity maintained during the test point. The results indicate that the motor leakage flow is dependent upon the motor

inlet pressure and the motor velocity. The relationship, empirically determined, was

$$q_3 = M_2 P_1 + L_2 \omega_1 + Z$$
.

A graph of the results of the pump leakage for minimum internal clearance is shown in Fig. A-1 as an example of the results obtained. A complete set of the results obtained is shown in reference one. A similar result is reported in the works cited in the bibliography.

The leakage parameters associated with the minimum clearance conditions are

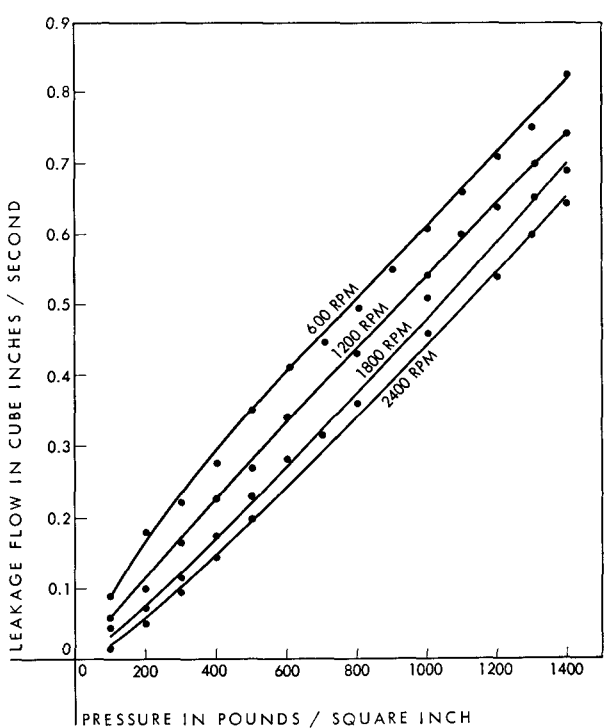
$$M_1 = 5.18 \times 10^{-4} \text{ in}^5/\text{lb-sec}$$

 $M_2 = 1.63 \times 10^{-4} \text{ in}^5/\text{lb-sec}$
 $L_1 = -3.18 \times 10^{-4} \text{ in}^3$
 $L_2 = 3.18 \times 10^{-4} \text{ in}^3$
 $Y = 0.05$
 $Z = 0.05$

The leakage parameters associated with the maximum clearance conditions are

$$M_1$$
=2.11×10⁻³ in⁵/lb-sec
 M_2 =3.11×10⁻³ in⁵/lb-sec
 L_1 =1.191×10⁻³ in³
 L_2 =-1.59×10⁻³ in³
 Y =0.14
 Z =0.28

Figure A-1 Pump leakage curves.



Appendix IV: Determination of the oil properties

The hydraulic fluid used throughout the experimental portion of this paper was Socony-Mobil Velocite "S" oil at 110°F. The value of the viscosity and the density may be obtained from the manufacturer. The value of the bulk modulus was determined experimentally by measuring the time required for a hammer blow-produced pressure impulse to pass from one dynamic pressure transducer section to a second one separated by a straight column of oil of several lengths. The bulk modulus was determined by the equation

$$B = \frac{L^2 \rho}{t^2}$$

where L is the distance between the stations and t is the time for the impulse to pass from one station to the other. The result of 2.0×10^5 psi was found for each length tested within 3 percent.

Acknowledgments

The author acknowledges the initial support of this study by Messrs. H. P. Wicklund, D. K. Rex and H. A. Panassidi, and the support and encouragement of Dr. R. E. Swanson and Mr. B. J. Greenblott in the preparation of the manuscript. Also he wishes to thank Dr. R. M. Evan-Iwanowski for his invaluable guidance and counseling.

The following notation has been used throughout this paper:

Symbol	Description	Units
a	a constant equal to V_1J/Bd_1	in ³ -sec ²
\boldsymbol{A}	Area	in^2
$(A_1, A_2, A_3, \& A_4)$	arbitrary constant	None
b	a constant equal to $\frac{(M_1+M_2)J}{d_1} \frac{V(K_1+2K_2)}{B}$	in³-sec
В	bulk modulus of the oil	lb/in ²
c	a constant equal to $(K_1+K_2')M_1+d_1+L_2$	in ³
C	velocity of sound in the oil	in/sec
d	volumetric displacement	in ³ /Rad
d_0	volumetric displacement of the pump	in ³ /Rad
d_1°	volumetric displacement of the pump	in ³ /Rad
e^{i}	universal constant (equal to 2.718)	None
f	a constant equal to $q_0 - (L_1W_0 + Y + Z)$	in ³ /sec
, J	load inertia	in-lb-sec ²
K_1	motor friction coefficient	lb-sec/in ²
K_2	hydraulic friction coefficient	lb-sec ² /in ²
K' ₂	linearized hydraulic friction coefficient	lb-sec/in ²
L^2	length	in
L_1	pump velocity leakage coefficient	in ³
$\stackrel{L_1}{L_2}$	motor velocity leakage coefficient	in ³
M_1	pump pressure leakage coefficient	in ⁵ /lb-sec
$M_1 \\ M_2$	motor pressure leakage coefficient	in ⁵ /lb-sec
P	pressure	lb/in ²
P_1	pressure in volume V_1	lb/in ²
$\stackrel{\scriptstyle I}{P}_2$	pressure in volume V_1	
$_{_{_{_{_{_{_{_{_{_{_{_{_{_{_{_{_{_{_$	motor friction pressure loss	lb/in²
	-	psi
P_{VL}	valve pressure losses flow	psi :3/
q		in ³ /sec
q_0	pump flow motor flow	in ³ /sec
q_1		in ³ /sec
q_2	pump leakage flow	in ³ /sec
q_3	motor leakage flow	in ³ /sec
t T	time	sec
<i>T</i>	torque	in-lb
v V	velocity	in/sec
•	volume	in ³
V_1	volume enclosed between the pump outlet and motor inlet	in ³
${V}_2$	volume enclosed between the motor outlet and the valve	in ³

Symbol	Description	Units
X	displacement or length	in
Y	constant	in ³ /sec
\boldsymbol{Z}	constant	in³/sec
ρ	mass density of the oil	$\frac{\text{lb-sec}^2}{\text{in}^4}$
au	time constant	sec
ω_0	pump angular velocity	Rad/sec
ω_1	motor angular velocity	Rad/sec
ω_1^F	final motor angular velocity	Rad/sec
ω_c	underdamped frequency	sec ⁻¹
$\omega_{m{d}}$	damping coefficient	sec-1
ωδ	overdamped frequency	sec ⁻¹

Bibliography

G. Recthof, C. Goth, H. Kord, "Thermal Effects in the Flow of Fluids Between Two Parallel Flat Plates in Relative Motion." A publication of Vickers Inc., 1958.

D. K. Crockett, "A Study of Performance Coefficients of Positive-Displacement Hydraulic Pumps and Motors, M.S. Thesis M.I.T., 1952.

S. C. Titcomb, "Analysis of the Performance of Hydraulic Spur Gear Devices," *IBM Tech. Report TR 01.15 032 559* March 1959.

R. C. Binder, Advanced Fluid Mechanics, Volume I, Prentice Hall, Inc., 1958.

R. Von Mises, Mathematical Theory of Compressible Fluid Flow, Academic Press, 1958.

Y. Chu and L. A. Gould, "Analogies for Hydraulic and Electric Drives in Servo-Mechanisms," J. ASME, July 1953. W. Thompson, Laplace Transformation, Prentice Hall, Inc., 1950.

Footnotes and references

- 1. W. Ernst, Oil Hydraulic Power and Its Industrial Applications, McGraw-Hill, 1949.
- The development of the "wave equations" is based on a similar analysis in Binder (op. cit.).
- 3. C. R. Wylie Jr., Advanced Engineering Mathematics, McGraw-Hill, 1951.

Received June 22, 1960